UNIVERSITY OF LIVERPOOL

Life703 Research Project

Final Report

Mapping BCAA Metabolic Adaptations to Resistance Training in Aging Muscle: A Cytoscape-Based Network Analysis

Shikha saini
201827340

Dr Masoud Isanejad

MSc Bioinformatics

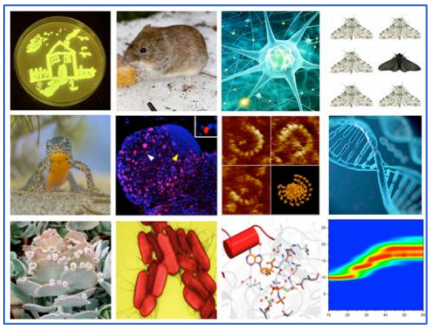

School of Biosciences

GAI Declaration

I **did / did not** (delete as appropriate) use GAI in the preparation of this report.

If you declare you **did** use GenAI, you must then provide the following information for each GenAI tool that you used.

- Name and version of GenAI tool
- Publisher (company that made the GenAI tool)
- URL of the GenAI tool
- Brief description of what the tool was used for, and how

Tool Details	Description of what used for, and how
ChatGPT,ScholarGPT	I used AI chatbots to assist in summarising results, refining language, and reducing word count to meet scientific publication standards.

* You may wish to revisit the university guidance on acceptable and unacceptable uses of GenAI that can be found here:
https://canvas.liverpool.ac.uk/courses/78922/pages/assessment

1. Lay Summary

As people age, they often lose muscle mass and strength sarcopenia. Exercise especially resistance training can help, but not everyone benefits the same way. In our study, we measured many metabolites in muscle before and after training to see how chemistry inside muscle changes. Using trusted network software Cytoscape, we mapped how these metabolites connect to genes and pathways and how they move together. We found that training shifted the overall muscle metabolic profile, though some overlap remained between before and after training, showing that changes were meaningful but not complete. Many molecules changed significantly, especially amino acids and energy-cycle compounds. I focused on branched-chain amino acids (BCAAs) which fuel and signal muscle growth. Because of its established metabolite-gene-enzyme-reactions, I used this Pathway to check whether Cytoscape could confirm known biological findings using only metabolite measurements and literature. From muscle samples before and after resistance training, Cytoscape pathway networks mapped 20 BCAA-related metabolites together with their linked genes and enzymes. After training, valine increased the most, while N-acetyl-L-glutamate and succinic anhydride decreased, pointing to a shift in BCAA and connected energy pathways. A correlation network showed leucine, isoleucine, valine, and 5-oxoproline rose and fell together, suggesting coordinated regulation and tightly linked metabolism of BCAA.
Overall, this work demonstrates that Cytoscape provides a dependable, reproducible way to compare pre- and post-training metabolism, confirm known pathways, and generate new, testable ideas to guide future muscle-health research.

2. Abstract

Aging-associated muscle decline (sarcopenia) is partly driven by disruptions in metabolic and genetic pathways. This study applies a network-based approach centred on Cytoscape, a free open-source platform with an extensive plugin ecosystem and beginner-friendly tutorials, to learn and deploy reliable workflows for pathway and network analysis of multi-omics data. Using the MetScape app in Cytoscape, which integrates KEGG content, we will construct metabolite–gene interaction and pathway networks from LC-MS metabolomics data. To validate the methodology, established BCAA metabolic reactions are used as a benchmark to confirm Cytoscape's capacity to both reproduce known biological interactions and generate novel hypotheses from experimental data. Using Cytoscape, we constructed detailed metabolite-gene interaction networks allowing comprehensive visualization and direct comparison of regulatory network changes. To capture coordinated metabolite behaviour, we will also build correlation networks using MetScape correlation workflow (including DSPC-based modelling and flexible thresholds), which supports both known and unknown metabolites for robust co-variation analysis. Statistical analyses revealed significant shifts in metabolites and gene expression after RT. By developing hands-on proficiency in Cytoscape’s documented workflows and leveraging its actively maintained ecosystem, this study establishes a reproducible, reliable framework for BCAA-centric network analysis in sarcopenia research and hypothesis generation for therapeutic targets.

3. Introduction

Sarcopenia, the progressive loss of skeletal muscle mass and strength with aging, is a major contributor to frailty, disability, and reduced quality of life in older adults.(Zuo et al., 2025) While resistance training (RT) is the most effective non-pharmacologic strategy to counteract this decline, responses are highly variable; some individuals experience robust hypertrophy and functional gains, whereas others show only modest improvement. Understanding the molecular determinants of this heterogeneity is essential for developing personalized interventions.

Metabolomics provides a systems-level snapshot of the biochemical state of muscle and can reveal pathways that are most responsive to exercise.(Patti et al., 2012, Wishart, 2019) Recent untargeted liquid-chromatography–mass spectrometry (LC-MS) studies have identified thousands of metabolites altered by RT, yet the integration of these data with gene and enzyme networks remains limited.(Zhou et al., 2012) Branched-chain amino acids (BCAAs) pathways are of particular interest because they directly regulate mTORC1 signalling, mitochondrial oxidative metabolism, and have been implicated in both muscle protein synthesis and sarcopenia progression. Using the well-characterized BCAA pathway as a biological benchmark, this study illustrates Cytoscape's ability to validate canonical reactions and, via flexible visualization and plugins such as MetScape, to generate novel, data-driven hypotheses.(Zuo et al., 2025)

Applying this workflow to the BCAA pathway, we mapped 20 input metabolites alongside related genes and enzymes. After RT, valine was the most upregulated metabolite, whereas N-acetyl-L-glutamate and succinic anhydride were most downregulated, indicating remodelling of BCAA flux. Furthermore, Correlation network analysis revealed strong positive correlations among leucine, isoleucine, valine, and 5-oxoproline, indicating coordinated regulation of BCAA metabolism (Rosato et al., 2018, Ian R. Lanza, 2010). Biologically, increased valine with tight BCAA co-regulation is consistent with enhanced BCAA trafficking/oxidation during remodelling, (Gagandeep Mann, 2021) while decreased N-acetyl-L-glutamate suggests shifted nitrogen handling and urea cycle post-training (Neinast et al., 2019) reduced succinic anhydride aligns with increased TCA flux and lower acylation pressuring,(Adegoke et al., 2012) , highlighting Cytoscape's power in uncovering complex metabolic relationships.(Shannon et al., 2003) This work establishes a reliable reproducible framework for network analysis, showcasing Cytoscape as an indispensable tool for developing targeted biomarker and therapeutic strategies (Zhang et al., 2013, Patti et al., 2012)

4. Methods

4.1 Data Preprocessing and Statistical Analysis

I have Receive the meta data including identified metabolites from LC- MS Data. The resulting feature table was imported into MetaboAnalyst (v6.0) for further quality control and normalization (Pang et al., 2024, Pang et al., 2022). To correct for sample variability, data normalization was performed using both the sum and probabilistic quotient normalization (PQN) methods both approaches were assessed for best performance based on total ion current inspection and QC sample clustering (Lu et al., 2023)

Subsequently, log2 transformation was applied to stabilize variance, and feature filtering was conducted to eliminate low-quality or low-abundance variables based on minimum intensity thresholds, presence in QC samples, and a minimum frequency present in at least 80% of samples per group then imported the normalized data file.(Pang et al., 2022)

Principal Component Analysis (PCA) and Partial Least Squares Discriminant Analysis (PLS-DA) were used for dimensionality reduction, outlier detection, and visualization of underlying group separation and metabolic shifts (performed in R v4.3.2). PLS-DA models were validated using permutation testing and cross-validation to mitigate overfitting. (Di Guida et al., 2016)Statistical significance of individual metabolites was determined via T-tests with Benjamini-Hochberg FDR correction to control for multiple comparisons. Biological significance was defined by adjusted P-values (FDR < 0.05). Volcano plots and hierarchical clustering were used for data visualization. Also use Fold Change calculation to calculate percentage change in metabolites. (Xia and Wishart, 2011, Pang et al., 2022)

All statistical analyses were implemented using reproducible R (v4.3.2) code **(Github),** ensuring full analytic traceability.

Normalized metabolites were used for downstream pathway and network enrichment analyses, including the integration of differential gene/protein expression data. Network construction and visualization were performed in Cytoscape (with MetScape

v3.1), linking significant metabolites with genes reaction based on curated pathway databases (e.g., KEGG). (Karnovsky et al., 2012, Gao et al., 2010, Shannon et al., 2003)

4.2 Pathway and Network Analysis

To elucidate the molecular mechanisms underlying significant metabolic alterations, LC-MS peak data underwent a comprehensive analytic workflow. First, all detected features (retention time, m/z, and intensity) were subjected to MetaboAnalyst (www.metaboanalyst.ca), incorporating the Mummichog algorithm for pathway-based analysis. The input comprised the complete peak list, significance threshold (top 10% features, $p < 0.008$), and specified ion mode (positive).(Lu et al., 2023, Pang et al., 2024). Prior to mummichog analysis, raw LC-MS data were normalized, to reduce technical variability and enhance comparability across samples, as recommended in metabolomics best practices.(Di Guida et al., 2016)

Pathway libraries from KEGG and the Model Framework Network (MFN) human genome-scale models were selected. (Karnovsky and Li, 2020, Chong et al., 2018) Mummichog mapped detected features to putative metabolites and performed over-representation analysis, generating probabilistic associations to metabolic pathways. (Lu et al., 2023) KEGG compound IDs corresponding to significant m/z features were extracted from MetaboAnalyst results. (Karnovsky and Li, 2020)

Significant KEGG compound IDs were then imported into Cytoscape (v3.10.2) utilizing the MetScape (V3.1) plugin app for network analysis (Gao et al., 2010) using the "Build network via Pathways-based input" function, with the organism set to "Human.".(Karnovsky and Li, 2020) The analysis specifically queried the BCAA pathway ("Valine, leucine and isoleucine degradation"), and the network was constructed to display compounds, reactions, enzymes, and genes. The resulting network nodes represent metabolites, genes, or enzymes, while the edges depict metabolic reactions or functional associations, which are algorithmically constructed based on integrated database knowledge from sources like KEGG. The final network (Figure 5) provides a systems-level visualization of the metabolic and gene regulatory interactions and the node table was extracted as CSV for further analysis. (Karnovsky and Li, 2020, Gao et al., 2010)

Throughout, gene-metabolite associations were manually curated by reference to published pathway databases (KEGG, HMDB) and literature's, ensuring each metabolite was accurately linked to its relevant metabolic reactions, catallyzing enzymes, and corresponding genes, as is standard in current integrative metabolomics research workflows. (Lu et al., 2023, Liu et al., 2017)

For the BCAA-focused correlation network analysis, a peak intensity matrix was constructed. First, the list of relevant metabolites was exported from the node table of the previously generated BCAA pathway network in Cytoscape. A new data file was then manually structured, with each sample arranged as a separate row and each exported metabolite as a distinct column. File were imported into the CorrelationCalculator. Within the tool, log transformation and autoscaling were applied to stabilize variance and harmonize scales.(Xia and Wishart, 2011, Di Guida et al., 2016). Pearson correlation coefficients were computed across samples, inspected via heatmaps, and filtered using a fixed Pearson threshold metabolites lacking any correlations above threshold were excluded. Where appropriate, Debiased Sparse Partial Correlation (DSPC) was additionally estimated to infer direct associations.(Di Guida et al., 2016, Rosato et al., 2018). Filtered correlation results were dynamically imported into MetScape (v3.1) to generate correlation networks, with nodes as metabolites and edges encoding correlation sign and magnitude (visualized via colour and width mappings) (Gao et al., 2010, Karnovsky and Li, 2020). BCAA metabolites and related intermediates were annotated to facilitate interpretation. constructed network (Figure 6) shows hub degree, and module organization, supporting robust visualization of RT-induced co-regulation patterns in the BCAA pathway. (Gagandeep Mann, 2021)

5. Results

5.1 Statistical Analysis

RT caused quantifiable but varied remodelling of the muscle metabolome in elderly persons across various multivariate and univariate investigations. Although training-attributable variance is moderate in comparison to interindividual differences, Principal Component Analysis revealed a partial overlap between pre- and post-RT samples, with blue circles and yellow triangles clustering in partially distinct regions (Figure 1).(Zhou et al., 2012, Xia et al., 2009) In support of this, the volcano plot revealed several metabolites that exceeded the FDR-adjusted significance threshold (red points), such as important amino acids, TCA intermediates, and gut-derived metabolites that rose after RT, indicating strong pathway-level remodelling (Figure 2).(Xia and Wishart, 2011) PLS-DA produced a clear discrimination between pre- and post-RT profiles, in contrast to the softer separation seen by PCA. This suggests that a coordinated subset of metabolites captures a unique intervention signature and confirms significant, classifiable metabolic reprogramming attributable to RT (Figure 3).(Zhou et al., 2012, Szymanska et al., 2012) Together, these results support the report's conclusion that exercise elicits broad but incomplete metabolic adaptation in aging skeletal muscle while revealing a discriminant molecular fingerprint suitable for pathway enrichment and downstream network analysis.

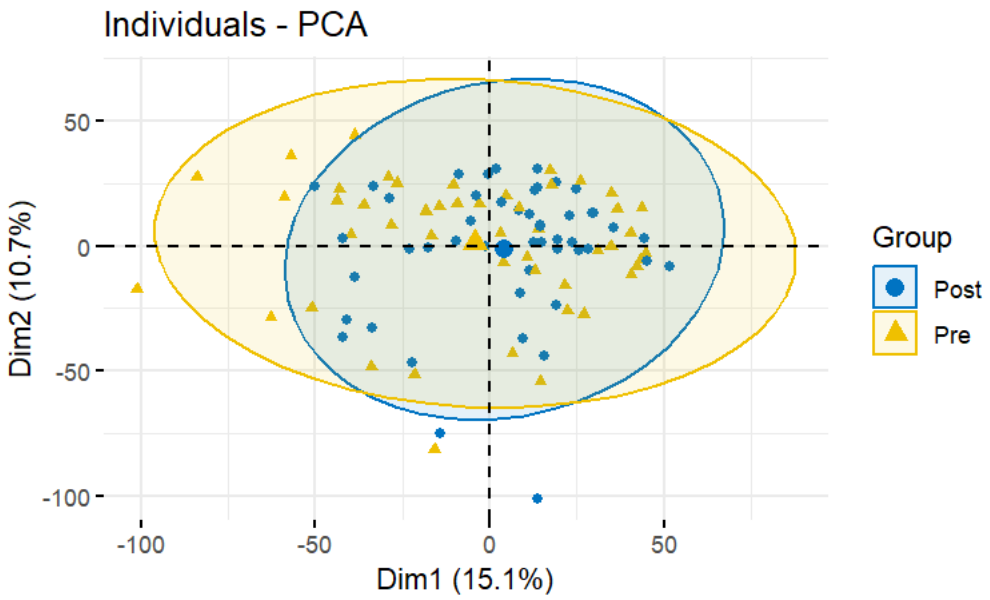

Figure 1: *The PCA plot shows the distribution of individual metabolomic profiles before (yellow triangles) and after (blue circles) resistance training. Each point represents a muscle biopsy sample, and the axes (Dim1/Dim2) capture the two largest sources of variation in the data. The ellipses encapsulate the spread of each group*

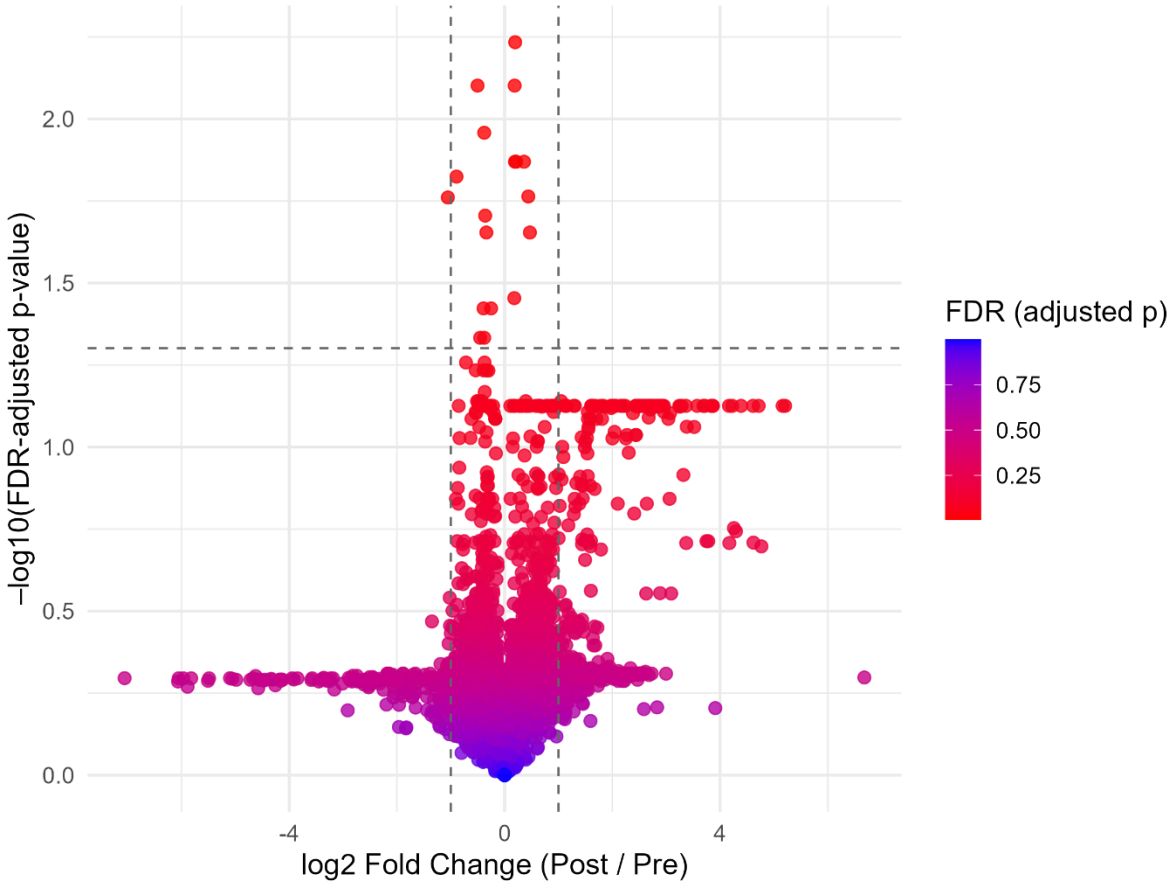

Figure 2: *The volcano plot displays the statistical significance (y-axis: -log10(p-value)) versus the magnitude of change (x-axis: log2 fold change) for each metabolite post- versus pre-training. Points further to the right (positive x-axis) are upregulated after training; those to the left are downregulated*

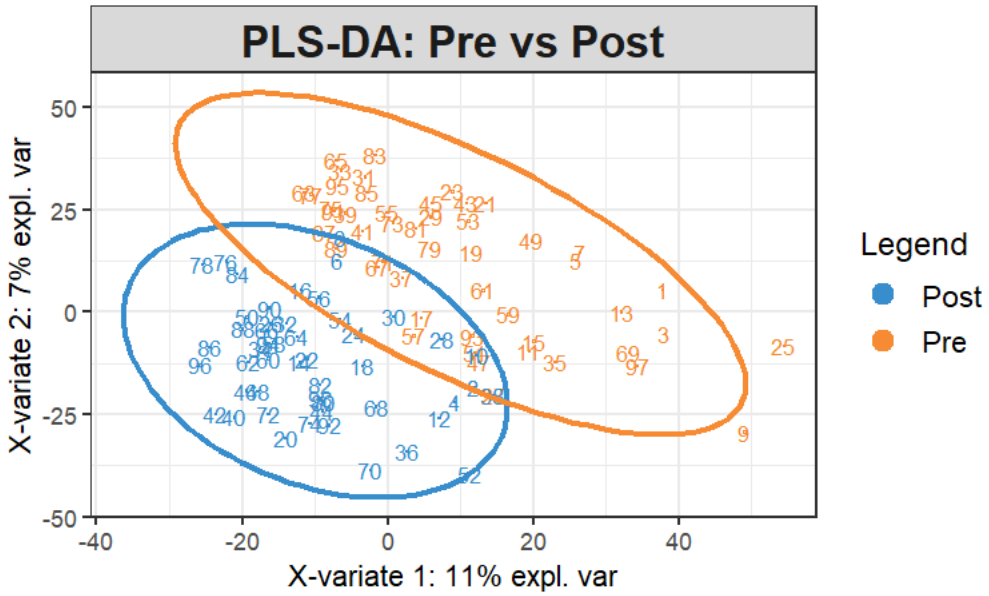

Figure 3: *The PLS-DA plot visually separates the pre- and post-training groups (orange and blue), with minimal overlap between the clusters. Each number represents an individual sample. The axes reflect latent variables explaining variance specifically attributable to group differences.*

5.2 Pathway and Network Analysis:

The untargeted LC-MS workflow detected 6,533 raw features across 122 Samples (pre- and post-resistance training). After intensity normalization, the top 10 % of features ($p < 0.008$) were submitted to MetaboAnalyst 6.0 for Mummichog pathway enrichment, which identified 54 significantly enriched pathways (FDR < 0.05) the Vitamin B6 (pyridoxine) metabolism showed the strongest association.(Lu et al., 2023, Pang et al., 2024) Given its metabolic relevance and broad literature presence, we focused on valine-leucine-isoleucine degradation pathway ($p = 2.1 \times 10^{-4}$, FDR = 0.012) for analysis which includes 20 matched metabolites, The metabolite list was subsequently exported for Cytoscape-based network analysis.(Shannon et al., 2003)

The MetScape-derived Compound-Reaction-Enzyme-Gene BCAAs interaction network (Figure 4) comprised 177 nodes (20 input metabolites, 43 additional compounds, 24 enzymes, 54 genes) linked by 260 edges.(Karnovsky et al., 2012) The layout emphasizes hub nodes such as the branched-chain aminotransferase complex and downstream enzymes, enabling visual comparison of pre- and post-resistance-training changes. The network visualisation thus integrates metabolite abundance, enzymatic activity, and gene expression into a single, interpretable map of BCAA metabolic remodelling. (Table 2). In parallel Cytoscape analysis of BCAA-related 20 input nodes create a metabolite-gene interaction network (Figure 5) The overlap between MetaboAnalyst/Mummichog pathway enrichment and Cytoscape compound–gene interaction mapping supports the reliability of the integrative workflow in capturing biologically meaningful BCAA metabolic remodelling. (Shannon et al., 2003, Pang et al., 2024) Key mapped compounds (Table 1) included valine-leucine-isoleucine degradation pathway input compound and intermediate with their KEGG IDs and directionality based on t-test results. Up-regulated leucine (C00123), valine (C00183), isoleucine (C00407), 3-methyl-2-oxobutanoic acid (C00141), and 4-methyl-2-oxopentanoate (C00233); down-regulated (S)-3-hydroxyisobutyrate (C06001) and (S)-methylmalonate semialdehyde (C06002) illustrated divergent BCAA catabolic fluxes. Directionality was annotated as “up-regulated,” “down-regulated,” or “variable” for cofactors such as FAD (C00016) and AMP (C00020).(Chen et al., 2017)

Comparative pre- vs. post-RT networks highlighted increased hub degree for BCAT2, BCKDHA/B, and ACADL, indicating enhanced mitochondrial BCAA oxidation and a shift toward oxidative metabolism (Table 2).(Zuo et al., 2025, Gagandeep Mann, 2021) Partial-correlation analysis (DSPC) matrix (Figure 6) confirmed positive co-regulation of leucine, valine, isoleucine, and 5-oxoproline, whereas AMP, (S)-3-hydroxyisobutyrate, and several dihydrolipoamide derivatives displayed inverse relationships, few moderate negative correlations link BCAA metabolites to citrate and 2-oxoglutarate, hinting at reciprocal shifts between amino-acid catabolism and TCA-cycle activity

Table 1: *List of 20 metabolites identified through Cytoscape network analysis in BCAAs and matched to mummichog pathway annotations with their corresponding KEGG compound IDs. The direction of change was determined from the training metadata using t-test–derived fold changes. Up-regulated metabolites were defined as FC > 1 with FDR < 0.05, while down-regulated metabolites were defined as FC < 1 with FDR < 0.05. Compounds labeled as variable showed fluctuations in both directions across samples and did not follow a consistent trend. Entries marked as slight change indicate minimal differences between pre- and post-training that did not meet significance thresholds.*

Canonical Name	**KEGG Compound ID**	**Direction of change**
FAD	C00016	Variable
AMP	C00020	Variable
Glutamate	C00025	Variable
2-Oxoglutarate	C00026	Variable
Leucine	C00123	Upregulated
3-Methyl-2-oxobutanoic acid	C00141	Upregulated
Acetoacetate	C00164	Slightly change
Valine	C00183	Upregulated
4-Methyl-2-oxopentanoate	C00233	Upregulated
2-Methyl-3-oxopropanoate	C00349	Upregulated
Isoleucine	C00407	Upregulated
Dihydrolipoamide	C00579	Upregulated
(S)-3-Methyl-2-oxopentanoic acid	C00671	Upregulated
Methylmalonate	C02170	Slightly change
3-Methyl-2-oxopentanoate	C03465	Upregulated
S-(2-Methylbutanoyl)-dihydrolipoamide	C05118	Slightly change
S-(3-Methylbutanoyl)-dihydrolipoamide	C05119	Slightly change
(S)-3-Hydroxyisobutyrate	C06001	Downregulated
(S)-Methylmalonate semialdehyde	C06002	Downregulated
2-methylglutaconic acid	CE5068	Upregulated

Table 2: *Metabolites-Genes of BCAAs identified through Cytoscape network analysis were mapped to known BCAA metabolic pathways functions and validated against resistance exercise studies. The table highlights how essential amino acids, catabolic intermediates, redox cofactors, and ROS by-products reflect enhanced BCAA oxidation in trained skeletal muscle and supporting literature evidence*

Metabolite / Gene	**Function in BCAA Metabolism**	**References**
BCAT1 / BCAT2 (branched-chain aminotransferases, cytosolic & mitochondrial)	First step: transamination of leucine, isoleucine, valine → α-ketoacids, boosting mitochondrial BCAA oxidation	(Gagandeep Mann, 2021)
BCKDHA / BCKDHB (branched-chain keto acid dehydrogenase, E1 α/β)	Irreversible oxidative decarboxylation of BCAA-derived ketoacids, greater valine/isoleucine catabolism	(Gagandeep Mann, 2021)
ACADs (acyl-CoA dehydrogenases: ACADL, ACADM, ACADS, IVD, etc.)	Oxidize acyl-CoA intermediates from BCAA breakdown, Upregulation of long-chain and branched-chain ACADs, enhancing fat & BCAA oxidation	Gagandeep Mann, S.M.
PCC (PCCA/PCCB) (propionyl-CoA carboxylase α/β)	Converts propionyl-CoA (from valine/isoleucine) → methylmalonyl-CoA, supports BCAA catabolite clearance	(Cordes and Metallo, 2021)
MCCC1 / MCCC2 (methylcrotonyl-CoA carboxylase)	Catalyzes leucine catabolism (3-methylcrotonyl-CoA → 3-methylglutaconyl-CoA), increases MCC activity, linked to leucine utilization	(Lerin et al., 2016)
HSD17B10 (17-β-hydroxysteroid dehydrogenase 10)	Mitochondrial enzyme for isoleucine breakdown (also in steroid metabolism)	(Marques et al., 2006)
ALDHs (aldehyde dehydrogenase family: ALDH2, ALDH3A1, ALDH7A1, etc.)	Metabolomic flux suggests ALDH upregulation in detox/oxidation pathways, Oxidize aldehydes from BCAA catabolites → acids	(Vassalli, 2019)
Leucine, Isoleucine, Valine	Essential BCAAs; leucine activates mTORC1	(Gagandeep Mann, 2021)
3-Methyl-2-oxobutanoic acid / 4-Methyl-2-oxopentanoate / 3-Methyl-2-oxopentanoate	BCAA-derived α-keto acids, marker of BCKDH activation	(Gagandeep Mann, 2021)
3-Methylcrotonyl-CoA → 3-Methylglutaconyl-CoA	Intermediates of leucine catabolism	(Alma L. Díaz-Pérez, 2016)
Methylmalonate / Propionyl-CoA → Succinyl-CoA	Valine/isoleucine catabolism feeding into TCA cycle	(Alma L. Díaz-Pérez, 2016)
Acetyl-CoA, Succinyl-CoA	Final products entering TCA cycle for ATP production	(Adegoke et al., 2012)
NAD+/NADH, FAD/FADH2	Cofactors required for BCAA oxidation enzymes	(Jeffrey T. Cole Ph.D., 2015)
H_2O_2, O_2^- (ROS markers)	Reactive by-products of BCAA catabolism	(Jiang et al., 2021)

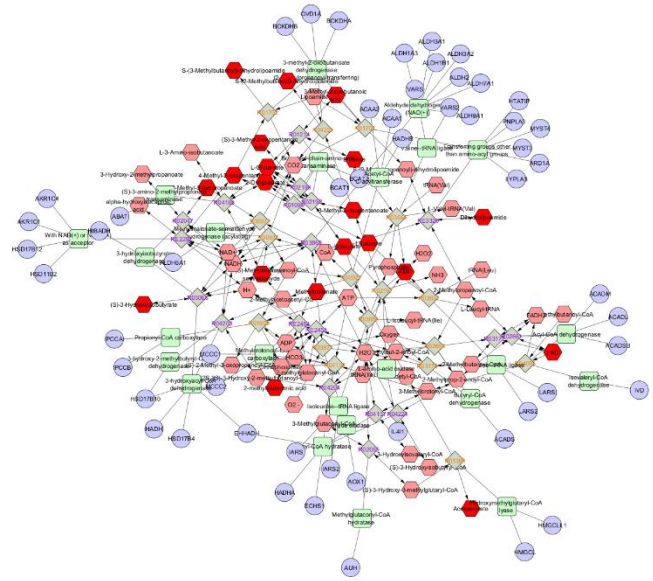

Figure 4: *Compound-Reaction-Enzyme-Gene network for BCAA metabolism generated in Cytoscape with MetScape. Pink hexagons: Metabolites, beige diamonds: Reactions, green squares: Enzymes, light-purple circles: Genes, red hexagons mark the Input LC-MS metabolites. Directed edges link compounds → reactions → enzymes → genes.*

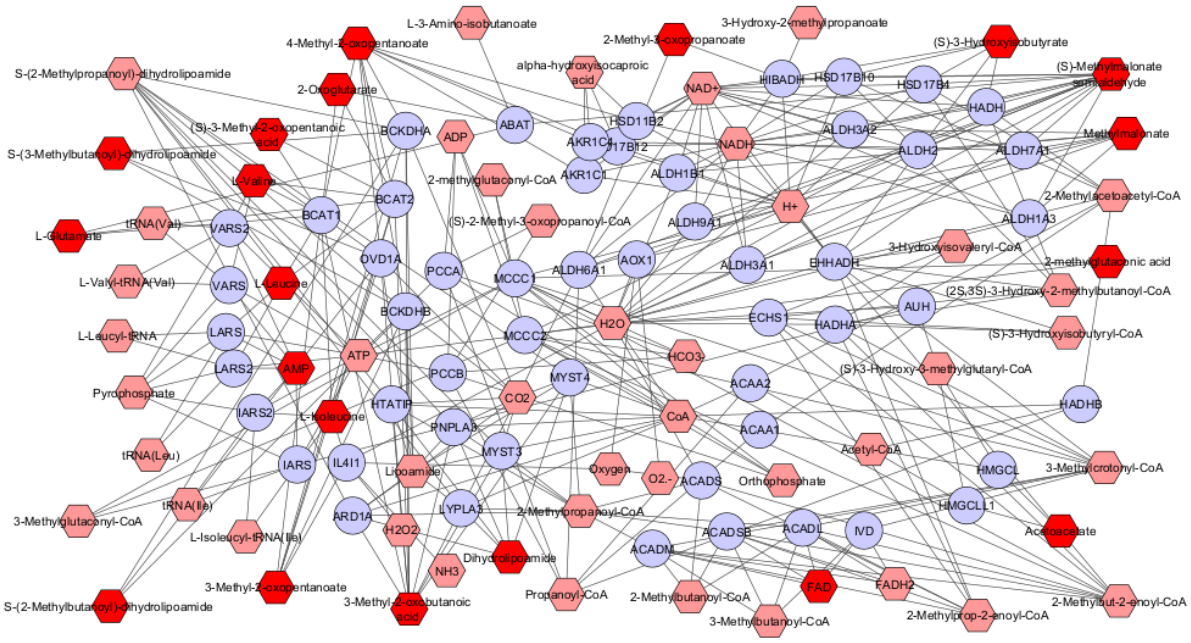

Figure 5: *BCAAs Metabolite-Gene pathway network generated in Cytoscape (MetScape). Pink hexagons denote metabolites (e.g., L-3-Amino-isobutanoate, 2-Oxobutanoate), light-purple circles represent genes (e.g., BCAT1, ALDH9A1), and red hexagons mark the input. Black lines indicate biochemical relationships (e.g., enzymatic reactions or regulatory links) between metabolites and genes.*

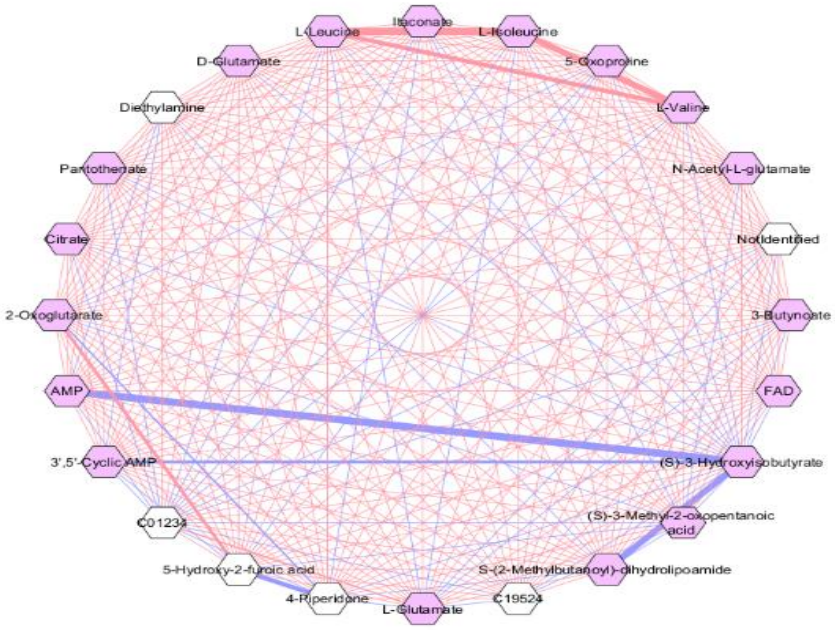

Figure 6: *Correlation matrix of BCAAs metabolites : Pink hexagons: identified compounds, white hexagons: unidentified features, Pink lines: positive correlation, blue lines: negative correlation and the thickness of lines indicate the strength like thick pink line is highly positive and blue is highly negative correlated.*

6. Discussion

Resistance training elicited broad yet incomplete remodelling of the aging muscle metabolome,(Zuo et al., 2025) with PCA showing partial overlap and PLS-DA revealing a discriminant intervention signature, indicating classifiable metabolic reprogramming despite substantial interindividual variability.(Lu et al., 2023) Pathway enrichment prioritized valine, leucine, isoleucine degradation, and Cytoscape networks mapped 20 BCAA-related metabolites with their reactions, enzymes, and genes, validating known biochemistry while enabling system-level comparisons.(Gao et al., 2010)Post-RT, valine increased most, whereas N-acetyl-L-glutamate and succinic anhydride decreased, consistent with altered BCAA flux, nitrogen handling, and TCA-linked energy metabolism.(Ian R. Lanza, 2010) Correlation and partial-correlation analyses showed tight positive co-regulation among leucine, isoleucine, valine, and 5-oxoproline, alongside inverse relationships with AMP and selective TCA intermediates, suggesting a coordinated shift toward mitochondrial BCAA oxidation and reciprocal tuning with central carbon metabolism(Rosato et al., 2018) Network features highlighted increased hub degree for BCAT2, BCKDHA/B, and ACADL, aligning with enhanced oxidative BCAA catabolism post-RT.(Gagandeep Mann, 2021, Zuo et al., 2025) Methodologically, Cytoscape/MetScape produced a reproducible workflow that confirmed known pathways, metabolites, genes, reactions and generated testable hypotheses from LC–MS data. Limitations include Mummichog maps features to putative metabolites, introducing identification uncertainty. Network construction relied on curated databases and manual curation, which may be incomplete or biased and correlation-based inference; targeted quantification, flux tracing, and enzyme activity assays will strengthen causal interpretation.(Rosato et al., 2018, Lu et al., 2023)

7. Conclusion

RT induces coordinated remodelling of BCAA and energy metabolism in aging muscle characterized by increased valine, decreased N-acetyl-L-glutamate/succinic anhydride, and strengthened BCAA co-regulation consistent with enhanced mitochondrial BCAA oxidation and adjusted nitrogen/TCA fluxes.(Zuo et al., 2025, Walvekar et al., 2018) The Cytoscape-based, multi-omics network framework is reliable and hypothesis-generating, supporting

biomarker discovery and therapeutic targeting for sarcopenia. Future work should prioritize targeted validation and functional assays within this integrative pipeline.

8. Acknowledgement:
I would like to express my deepest gratitude to my supervisor, **Dr. Masoud Isanejad**, for his invaluable guidance, continuous support, and constructive feedback throughout the course of this research. I am also sincerely thankful to **Ms. Ziyi Zhong**, Senior PhD student in our lab, for her generous help, guidance, and encouragement during various stages of this study. Finally, I wish to acknowledge the **University of Liverpool** for providing the resources, facilities, and academic environment that made this research possible.

9. Reference :

ADEGOKE, O. A., ABDULLAHI, A. & TAVAJOHI-FINI, P. 2012. mTORC1 and the regulation of skeletal muscle anabolism and mass. *Appl Physiol Nutr Metab,* 37**,** 395–406.

ALMA L. DÍAZ-PÉREZ, C. D.-P. J. C.-G. 2016. Bacterial l-leucine catabolism as a source of secondary metabolites. *Springer Nature*.

CHEN, L., ZHANG, Y. H., WANG, S., ZHANG, Y., HUANG, T. & CAI, Y. D. 2017. Prediction and analysis of essential genes using the enrichments of gene ontology and KEGG pathways. *PLoS One,* 12**,** e0184129.

CHONG, J., SOUFAN, O., LI, C., CARAUS, I., LI, S., BOURQUE, G., WISHART, D. S. & XIA, J. 2018. MetaboAnalyst 4.0: towards more transparent and integrative metabolomics analysis. *Nucleic Acids Res,* 46**,** W486–W494.

CORDES, T. & METALLO, C. M. 2021. Itaconate Alters Succinate and Coenzyme A Metabolism via Inhibition of Mitochondrial Complex II and Methylmalonyl-CoA Mutase. *Metabolites,* 11.

DI GUIDA, R., ENGEL, J., ALLWOOD, J. W., WEBER, R. J., JONES, M. R., SOMMER, U., VIANT, M. R. & DUNN, W. B. 2016. Non-targeted UHPLC-MS metabolomic data processing methods: a comparative investigation of normalisation, missing value imputation, transformation and scaling. *Metabolomics,* 12**,** 93.

GAGANDEEP MANN, S. M., GLORY MADU, OLASUNKANMI A J ADEGOKE 2021. Branched-chain Amino Acids: Catabolism in Skeletal Muscle and Implications for Muscle and Whole-body Metabolism. *Frontiers in Physiology,* 12-2021.

GAO, J., TARCEA, V. G., KARNOVSKY, A., MIREL, B. R., WEYMOUTH, T. E., BEECHER, C. W., CAVALCOLI, J. D., ATHEY, B. D., OMENN, G. S., BURANT, C. F. & JAGADISH, H. V. 2010. Metscape: a Cytoscape plug-in for visualizing and interpreting metabolomic data in the context of human metabolic networks. *Bioinformatics,* 26**,** 971–3.

IAN R. LANZA, S. Z., LAWRENCE E. WARD, HELEN KARAKELIDES, DANIEL RAFTERY, K.SREEKUMARAN NAIR 2010. Quantitative Metabolomics by 1 H-NMR and LC-MS/MS

Confirms Altered Metabolic Pathways in Diabetes.

JEFFREY T. COLE PH.D., M. S. 2015. *Metabolism of BCAAs*.

JIANG, Y. J., SUN, S. J., CAO, W. X., LAN, X. T., NI, M., FU, H., LI, D. J., WANG, P. & SHEN, F. M. 2021. Excessive ROS production and enhanced autophagy contribute to myocardial injury induced by branched-chain amino acids: Roles for the AMPK-ULK1 signaling pathway and alpha7nAChR. *Biochim Biophys Acta Mol Basis Dis,* 1867**,** 165980.

KARNOVSKY, A. & LI, S. 2020. Pathway Analysis for Targeted and Untargeted Metabolomics. *Methods Mol Biol,* 2104**,** 387–400.

KARNOVSKY, A., WEYMOUTH, T., HULL, T., TARCEA, V. G., SCARDONI, G., LAUDANNA, C., SARTOR, M. A., STRINGER, K. A., JAGADISH, H. V.,

BURANT, C., ATHEY, B. & OMENN, G. S. 2012. Metscape 2 bioinformatics tool for the analysis and visualization of metabolomics and gene expression data. *Bioinformatics,* 28**,** 373–80.

LERIN, C., GOLDFINE, A. B., BOES, T., LIU, M., KASIF, S., DREYFUSS, J. M., DE SOUSA-COELHO, A. L., DAHER, G., MANOLI, I., SYSOL, J. R., ISGANAITIS, E., JESSEN, N., GOODYEAR, L. J., BEEBE, K., GALL, W., VENDITTI, C. P. & PATTI, M. E. 2016. Defects in muscle branched-chain amino acid oxidation contribute to impaired lipid metabolism. *Mol Metab,* 5**,** 926–936.

LIU, X. L., MING, Y. N., ZHANG, J. Y., CHEN, X. Y., ZENG, M. D. & MAO, Y. M. 2017. Gene-metabolite network analysis in different nonalcoholic fatty liver disease phenotypes. *Exp Mol Med,* 49**,** e283.

LU, Y., PANG, Z. & XIA, J. 2023. Comprehensive investigation of pathway enrichment methods for functional interpretation of LC-MS global metabolomics data. *Brief Bioinform,* 24.

MARQUES, A. T., ANTUNES, A., FERNANDES, P. A. & RAMOS, M. J. 2006. Comparative evolutionary genomics of the HADH2 gene encoding Abeta-binding alcohol dehydrogenase/17beta-hydroxysteroid dehydrogenase type 10 (ABAD/HSD10). *BMC Genomics,* 7**,** 202.

NEINAST, M. D., JANG, C., HUI, S., MURASHIGE, D. S., CHU, Q., MORSCHER, R. J., LI, X., ZHAN, L., WHITE, E., ANTHONY, T. G., RABINOWITZ, J. D. & ARANY, Z. 2019. Quantitative Analysis of the Whole-Body Metabolic Fate of Branched-Chain Amino Acids. *Cell Metab,* 29**,** 417–429 e4.

PANG, Z., LU, Y., ZHOU, G., HUI, F., XU, L., VIAU, C., SPIGELMAN, A. F., MACDONALD, P. E., WISHART, D. S., LI, S. & XIA, J. 2024. MetaboAnalyst 6.0: towards a unified platform for metabolomics data processing, analysis and interpretation. *Nucleic Acids Res,* 52**,** W398–W406.

PANG, Z., ZHOU, G., EWALD, J., CHANG, L., HACARIZ, O., BASU, N. & XIA, J. 2022. Using MetaboAnalyst 5.0 for LC-HRMS spectra processing, multi-omics integration and covariate adjustment of global metabolomics data. *Nat Protoc,* 17**,** 1735–1761.

PATTI, G. J., YANES, O. & SIUZDAK, G. 2012. Innovation: Metabolomics: the apogee of the omics trilogy. *Nat Rev Mol Cell Biol,* 13**,** 263–9.

ROSATO, A., TENORI, L., CASCANTE, M., DE ATAURI CARULLA, P. R., MARTINS DOS SANTOS, V. A. P. & SACCENTI, E. 2018. From correlation to causation: analysis of metabolomics data using systems biology approaches. *Metabolomics,* 14**,** 37.

SHANNON, P., MARKIEL, A., OZIER, O., BALIGA, N. S., WANG, J. T., RAMAGE, D., AMIN, N., SCHWIKOWSKI, B. & IDEKER, T. 2003. Cytoscape: a software environment for integrated models of biomolecular interaction networks. *Genome Res,* 13**,** 2498–504.

SZYMANSKA, E., SACCENTI, E., SMILDE, A. K. & WESTERHUIS, J. A. 2012. Double-check: validation of diagnostic statistics for PLS-DA models in metabolomics studies. *Metabolomics,* 8**,** 3–16.

VASSALLI, G. 2019. Aldehyde Dehydrogenases: Not Just Markers, but Functional Regulators of Stem Cells. *Stem Cells Int,* 2019**,** 3904645.

WALVEKAR, A., RASHIDA, Z., MADDALI, H. & LAXMAN, S. 2018. A versatile LC-MS/MS approach for comprehensive, quantitative analysis of central metabolic pathways. *Wellcome Open Res,* 3**,** 122.

WISHART, D. S. 2019. Metabolomics for Investigating Physiological and Pathophysiological Processes. *Physiol Rev,* 99**,** 1819–1875.

XIA, J., PSYCHOGIOS, N., YOUNG, N. & WISHART, D. S. 2009. MetaboAnalyst: a web server for metabolomic data analysis and interpretation. *Nucleic Acids Res,* 37**,** W652–60.

XIA, J. & WISHART, D. S. 2011. Web-based inference of biological patterns, functions and pathways from metabolomic data using MetaboAnalyst. *Nat Protoc,* 6**,** 743–60.

ZHANG, A. H., SUN, H., HAN, Y., YAN, G. L., YUAN, Y., SONG, G. C., YUAN, X. X., XIE, N. & WANG, X. J. 2013. Ultraperformance liquid chromatography-mass

spectrometry based comprehensive metabolomics combined with pattern recognition and network analysis methods for characterization of metabolites and metabolic pathways from biological data sets. *Anal Chem,* 85**,** 7606–12.

ZHOU, B., XIAO, J. F., TULI, L. & RESSOM, H. W. 2012. LC-MS-based metabolomics. *Mol Biosyst,* 8**,** 470–81.

ZUO, X., ZHAO, R., WU, M., WANG, Y., WANG, S., TANG, K., WANG, Y., CHEN, J., YAN, X., CAO, Y. & LI, T. 2025. Multi-omic profiling of sarcopenia identifies disrupted branched-chain amino acid catabolism as a causal mechanism and therapeutic target. *Nat Aging,* 5**,** 419–436.